CONF-8910222--11

PERFORMANCE OF CONTAINMENT PENETRATIONS UNDER SEVERE ACCIDENT LOADINGS[1]

M. B. Parks
D. B. Clauss
Sandia National Laboratories
Albuquerque, NM 87185

SAND--89-1631C

DE90 003950

Abstract

The paper provides a summary of efforts to date to better understand the leakage behavior of containment penetrations when subjected to severe accident conditions. The research activities discussed herein are a part of the Containment Integrity Programs, which are managed by Sandia National Laboratories for the U.S. Nuclear Regulatory Commission. Past containment penetration research topics, which are briefly described, include testing of typical compression seals and gaskets, electrical penetration assemblies, and a personnel airlock, as well as an investigation of leakage due to ovalization of penetration sleeves. The primary focus of the paper is on recent or ongoing research programs on the behavior of inflatable seals, bellows, and of pressure unseating equipment hatches.

1.0 INTRODUCTION

Since the incident at Three Mile Island, an increased emphasis has been placed on understanding the consequences of accidents that produce pressure and temperature conditions within containment that exceed the design basis. Because the containment is the last engineered barrier to the release of radioactive material, an accurate estimate of the containment's ultimate capacity is essential in order to develop accident management strategies.

Sandia National Laboratories is conducting several research programs to develop test validated methods for the prediction of the ultimate pressure capacity, at elevated temperatures, of light water reactor (LWR) containment structures. These research programs, which are collectively known as the Containment Integrity Programs, are sponsored by the U. S. Nuclear Regulatory Commission (NRC).

The containment pressure boundary includes not only the shell but also numerous mechanical and electrical penetrations, each of which provide a potential leak path through containment. The final goal of the Containment Integrity Programs is to develop methods to predict the ultimate pressure and temperature conditions for each possible failure mode, whether it is a shell failure or failure of one of the penetrations. The ultimate capacity of the containment pressure boundary could then be estimated as the lowest failure pressure of the potential failure modes.

---

1. This work was supported by the U.S. Nuclear Regulatory Commission and performed at Sandia National Laboratories, which is operated by the U.S. Department of Energy under contract number DE-AC04-76DP00789.

As a part of the Containment Integrity Programs, a series of scale model containment tests have been performed including a 1:8-scale steel model and a 1:6-scale reinforced concrete model [1-7]. Because of the reduced scale and limited number of tests, the model tests could not include all of the various penetration designs. Thus, several separate test programs have been conducted in which various features of containment penetrations were tested in order to determine their leakage behavior when subjected to severe accident conditions. Past containment penetration research programs have included testing of typical compression seals and gaskets, electrical penetration assemblies (EPAs), and a personnel airlock. Also, an investigation of leakage due to ovalization of penetration sleeves was conducted in conjunction with the scale model tests. A brief review of each of these programs is provided in Section 2. A study of the performance of containment isolation valves, which was also sponsored by the NRC, has been conducted at Idaho National Engineering Laboratory (INEL) [8].

Recently, a series of tests were conducted to determine the leakage behavior of inflatable seals when subjected to postulated severe accident combinations of containment pressure and temperature. Also, there is an ongoing research activity to determine the capacity of bellows that are used at some containment penetrations. Further testing of the pressure-unseating equipment hatch in the 1/6-scale reinforced containment model is also underway. Section 3 provides a description of each of these programs. Finally, a brief summary of the containment penetration programs is presented in Section 4.

2.0 PAST CONTAINMENT PENETRATION RESEARCH PROGRAMS

2.1 Compression Seals and Gaskets

Compression seals and gaskets form an important part of the containment pressure boundary in many operable penetrations, such as equipment hatches, personnel locks, and drywell heads. If metal-to-metal contact does not exist between the sealing surfaces of these penetrations, the gaskets represent the only barrier to prevent leakage through the containment boundary at these locations.

Severe accident testing of typical gasket cross-sections and materials has been conducted at Sandia [9] and at INEL (under contract to Sandia) [10]. The tested seals were made from either ethylene propylene (EPDM), silicone, or neoprene. Unaged and aged (thermal only or thermal plus radiation) gaskets were included in the test programs. Steam, heated dry air, or heated dry nitrogen were used to supply the test environments. During these tests, the gaskets were subjected to constant internal pressure (either 143 or 160 psig) while the seal temperature was slowly increased up to as much as 700°F. A general summary of the test results obtained both at Sandia and INEL is provided in Table 1.

For each test, seal "failure" was recorded as the temperature at which significant leakage past the seals began. After testing, many of the gaskets were charred and were of a powdery consistency as if combustion of the gasket material occurred during the tests.

The test results indicated that the failure temperature was independent of applied aging, gap between sealing surfaces, or rotation of the sealing surfaces.[2] As shown, silicone appears to have a lower failure temperature in a steam environment than in air or nitrogen whereas EPDM was not strongly affected by the applied test environment.

Table 1
Summary of Compression Seal Test Results

Material	Number of Tests	Test Environment	Range of Failure Temperatures (°F)	Mean Failure Temperatures (°F)
EPDM	5	Steam	626-669	647
	8	Nitrogen	577-667	613
	1	Air	651	651
Silicone	8	Steam	486-592	512
	2	Nitrogen	>700	>700
	1	Air	681	681
Neoprene	3	Nitrogen	460-500	487

It should be noted that, for all test results in Table 1, a fixed gap was imposed between the metal sealing surfaces. A few tests were also conducted in which there was metal-to-metal (no gap) contact of the sealing surfaces. As might be expected, no leakage was usually observed for these tests up to the maximum test temperature of 700°F.[3] More detailed information regarding the test conduct and results is available in the final test reports [9,10].

2.2 Electrical Penetration Assemblies

Electrical penetration assemblies (EPAs) are used to provide a leak-tight pass-through in nuclear containment buildings for electrical cables with power, control, and instrumentation applications. Typical pressurized water reactor (PWR) and boiling water reactor (BWR) containments include anywhere from 30 to 70 EPAs per unit [11,12].

Three EPA designs - one each by Conax, D. G. O'Brien, and Westinghouse - were tested as a part of the Electrical Penetration Assemblies Program at Sandia. These three EPAs provide a good representation of the different seal materials used and applications for containments of all major reactor types. The EPA test specimens were subjected to a

2. However, aging tends to reduce the available gasket springback which may effect the leakage behavior of some containment penetrations as described in Section 3.3.

3. The test fixtures were fabricated to close tolerances to ensure that the metal sealing surfaces were flat. Any out-of-flatness of the sealing surfaces in an actual penetration could prevent metal-to-metal contact and thus, should be considered when estimating leakage.

combination of radiation and thermal aging to simulate end of service life conditions. After aging, each EPA was exposed to "worst-case" severe accident conditions representative of the containment type in which they are most commonly employed. Table 2 provides a list of the accident conditions applied during testing.

The conditions listed in Table 2 were applied for a period of 10 days. Detectable leakage was not measured during any of the tests. The temperature distribution and electrical continuity of each EPA was also monitored during the tests. Because there are a large number of different EPA designs, the exceptional leak integrity of the three EPAs in this test program should not be assumed to necessarily apply to all designs. EPAs manufactured before 1971 were not regulated by any national codes or standards and were often fabricated in the field, whereas EPAs tested in this program were subject to rigorous quality assurance and were designed to meet the standards of IEEE 317-1976 and IEEE 323-1974.

Table 2
Summary of EPA Test Conditions

EPA Design	Containment Type	Maximum Accident Loads
D.G. O'Brien	PWR	361°F, 155 psia
Westinghouse	BWR Mk-III	400°F, 75 psia
Conax	BWR Mk-I	700°F, 135 psia

However, given information on the containment pressure and temperature conditions, a heat transfer analysis to determine the approximate temperature profiles in the EPA, and the proper exercise of engineering judgement, a reasonable evaluation of the leakage potential of other EPA designs can be made. The above tests provide a good basis for such an evaluation.

2.3 Personnel Airlocks

A full-size personnel airlock, which was originally fabricated for use in the cancelled Callaway Unit 2 reactor, has been tested by CBI Research Corporation under contract to Sandia. CBI Research Corporation has written a comprehensive data report for the tests [13].

"Double dog-ear" gaskets, constructed of EPDM E603 material, were used to provide a seal between each door and bulkhead. The gaskets were subjected to an accelerated aging process to simulate 40 years of service followed by a loss of coolant accident (LOCA). The airlock design pressure and temperature was 60 psig and 340°F, respectively. During one of the more severe tests, the inner door and bulkhead were subjected to a maximum external pressure of 300 psig and a maximum air temperature of 400°F. No leakage occurred during this test.

During the final test, the inner door temperature was held at approximately 650°F for two hours at ambient pressure. For these conditions the air temperature inside the door was >800°F. Upon increasing the pressure on the inside of the inner door to about 150 psig, significant leakage began past the inner door. However, because the outer door temperature was much lower, these seals were still intact and thus, no leakage occurred past the outer door even for these extreme conditions. As predicted by pretest finite element analyses, the structural behavior of the airlock was essentially elastic for all tests.

The seal failure conditions, 650°F and 150 psig, agree quite well with the failure temperatures observed during the seals and gaskets test program presented in Section 2.1. The posttest condition was also similar in that the seals appeared charred as if combustion of the seal material had occurred.

It should be noted that other airlock designs may be less stiff than the test specimen; thus, deformation of the sealing surfaces could be substantially larger than in the tested airlock. Because of the complex interaction between the door, bulkhead, and gasket, detailed 3-D finite element analysis may be required to accurately predict the response of different airlock designs.

2.4 Leakage Due to Ovalization of Penetration Sleeves

For penetrations in which the sleeve forms an integral part of the sealing surface, as is the case in many equipment hatch designs, leakage may occur due to ovalization of the sleeve. Ovalization will occur in cylindrical containments provided that: 1) there is no significant restraint along the length or at the ends of the penetration sleeves, such as bulkheads or welded covers, and 2) there is no significant variation of the inside radius of the containment in the vicinity of the penetration, such as an inward projecting boss. If these conditions are met, the horizontal diameter of the sleeve increases due to internal pressurization of the containment while the vertical diameter decreases by an equal amount at the sealing surfaces.

Results of the 1/8-scale steel containment [14] and the 1/6-scale concrete containment model tests indicate that the amount of ovalization can be calculated as simply the circumferential membrane free-field strain at the sleeve elevation times the sleeve radius. Leakage can be expected to occur when the amount of ovalization equals the sleeve thickness.

3.0 RECENT ADVANCES

3.1 Inflatable Seals

This section provides a review of inflatable seals applications, a description of the test program, and then presents test validated analytical methods to predict the containment pressure and temperature conditions at which leakage would be expected for a given seal pressure.

3.1.1 Background Information

Inflatable seals are used to prevent leakage around the perimeter of personnel and escape lock doors in approximately 10% of U.S. containments. All of the installations are in either PWR or BWR Mark-III type containments. They are fastened to the outer edge of the airlock doors and, when pressurized with air, seal the gap between the door and the bulkhead. When deflated, there is a 3/8-inch gap between the sealing surface of the seals and the bulkhead. A typical application is shown in Figure 1. The airlock doors are rectangular with "rounded" corners and vary in size from 8'-0" X 5'-0" to 6'-6" X 3'-6". Typically the corner radius is about 12 inches.

Because of the relatively large 3/8-inch gap that exists between the seals and the bulkhead around the entire perimeter of the door if the seals are deflated, it is important to understand the air supply system for each seal. The pressure inside the seal is furnished by the instrument air supply system. A schematic of a typical air supply system for each seal is provided in Figure 2. If the instrument air supply is lost, a check valve ensures that the accumulator tank and the seal remain pressurized at the normal system pressure level. As shown, an air pressure accumulator tank is also placed in the air supply line. The accumulator tank is large enough to repressurize the seals to the approximate normal operating pressure a few times thus enabling the airlock doors to be opened and then closed and resealed in the event of a loss of the instrument air supply system.

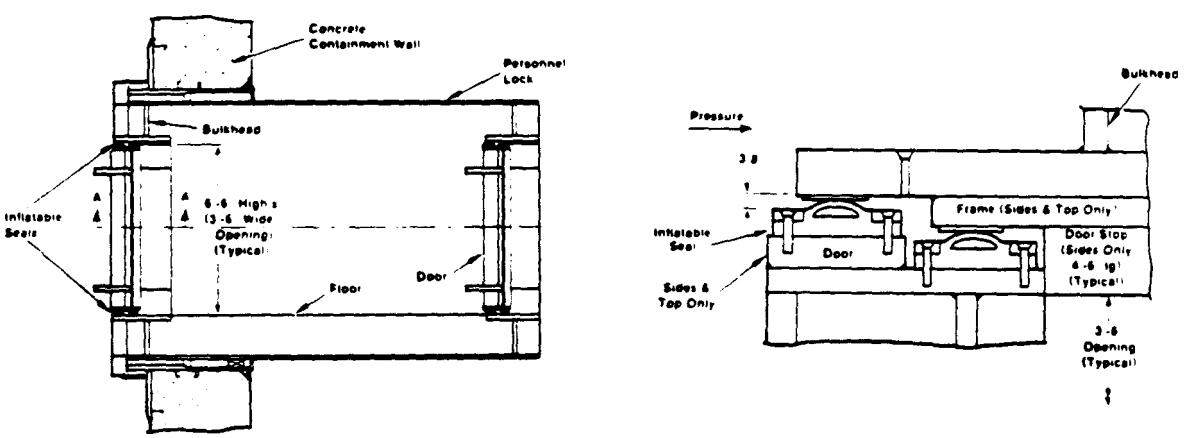

(a) Elevation View (b) Section A-A

Figure 1. Typical Application of Inflatable Seals in Personnel Airlock Doors (Note that seals are shown fully inflated.)

There is also an inflation valve between each accumulator tank and inflatable seal. During the planning and execution of the inflatable seals tests, it was believed that, once the seals are inflated, they are isolated from their pressure source by closing the inflation valve. (This information was obtained from an expert in the use of inflatable seals in nuclear containments.) In this way, increasing containment pressure, which acts on the seals as an external "side" pressure, and increasing seal temperature produce a corresponding increase in the seal pressure. The effect of increasing seal pressure is to

prohibit leakage past the seals until a higher containment pressure than would occur if the seal pressure remained constant. The majority of the inflatable seals tests modeled the above condition in which the seals are isolated from their pressure source after inflation.

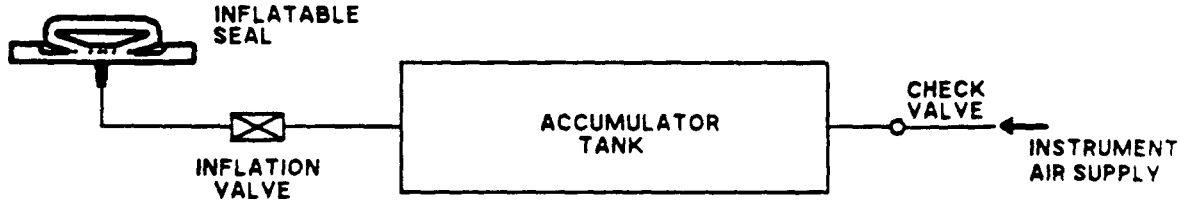

Figure 2. Typical Instrument Air Supply System for Each Seal

After completion of all inflatable seals tests, it was discovered during a plant tour that the above inflation valve actually remains open during normal operation such that an open pathway for the flow of air exists between each seal and accumulator tank. In this way, increasing containment pressure has an insignificant effect on the seal pressure. However, because both the accumulator tank and seal are exposed to the same containment environment, increasing containment temperature will still produce a corresponding increase in seal pressure. (Based on the test results, it was determined that the increase in seal pressure due to temperature can accurately be predicted using the ideal gas law.)

The above "revised" description of the function of the inflation valve is believed to be representative of all containments that use inflatable seals. Fortunately, tests were conducted which modeled not only the first valve condition in which the seals are isolated from their pressure source but also the second condition in which the seal pressure remains constant for increasing containment pressure.

According to instructions from the supplier, the seal pressure must be at least 30 psi greater than the containment design pressure in order to ensure that leakage does not exceed design allowables. A survey of the plants that are currently using inflatable seals revealed that the normal operating seal pressure varied from plant to plant with a minimum seal pressure of 50 psig and a maximum of 110 psig. In all cases, the seal pressure is at least 30 psi greater than the containment design pressure.

During a review of the applications of inflatable seals, it was determined that three different designs of inflatable seals are currently available for use in nuclear containments: an "old" design (Figure 3(a)), a "new" design (Figure 3(b)), and a modification of the old design. In some cases, the old design was found to have undesirably high amounts of leakage when compared to design allowable leak rates. In order to improve the leakage behavior, a 1/8-inch thick layer of EPDM E401 material was added to the sealing surface. The seals already fabricated using the old design were modified by vulcanizing a 1-1/2-inch wide by 1/8-inch thick layer of EPDM E401, 40 durometer material to the sealing surface. For the new design seals, the added E401 material is incorporated as an integral part of the seal as illustrated in Figure 3(b). This type of seal is currently supplied for use in nuclear containments. It should be noted that,

other than the added E401 layer, the seals are constructed of EPDM E603, 60 durometer material with Kevlar reinforcement.

Only the old and new design seals were included in the test program. The old design seals were included because they are still in use in some containments. The modified old design seals were not tested since they were only supplied for a short period of time and because their leakage behavior should be at least as good as that of the old design seals.

The test program was designed to determine the leakage behavior of inflatable seals when subjected to containment pressure and temperature conditions that are well beyond the seals design basis. External "containment" pressure was applied by placing the test fixture containing the inflatable seals inside a pressurized test chamber. Figure 4 presents a schematic of the test setup. The overall shape of the test fixture is that of a short length of cylinder with an outer diameter of approximately 36 inches and a length of approximately 13 inches. The plate to which the seals are attached is about 32 inches in diameter. Thus, the circumferential length of the tested seals is approximately 100 inches as compared to a total length of about 240 inches for a typical 6'-6" X 3'-6" personnel airlock door.

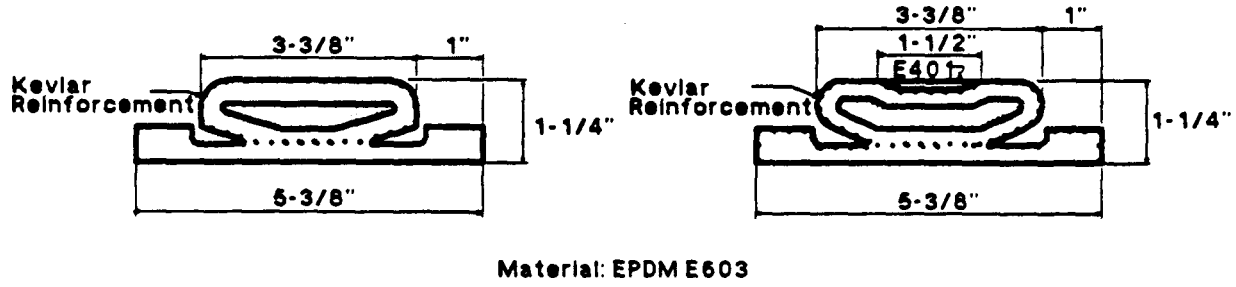

(a) "Old" Seal Design (b) "New" Seal Design

Figure 3. Cross-Sections of Two Primary Seal Designs Used in LWR Containments

3.1.2 Description of Inflatable Seals Test Program

The primary objective of the inflatable seals test program is to develop methods to predict the containment pressure and temperature, for a given normal operating seal pressure, at which significant leakage past inflatable seals will occur. The internal seal pressure and temperature, containment pressure, seal design, and applied aging conditions are parameters that were examined during the tests to determine their effect on the leakage behavior of inflatable seals.

As outlined in Table 3, a total of four different series of inflatable seals tests have been performed. The first two tests were of the old seal design whereas the last two tests were of the new design. For each type of seal, an unaged (Test series 1 and 3) and an aged (Test series 2 and 4) pair of seals were tested. For each test series, the seals were tested first at room temperature and then at elevated temperatures at or above 300°F. The test temperatures are based on estimates of the airlock seal temperature which would be caused by postulated BWR Mk-III or PWR severe accident conditions within the containment.

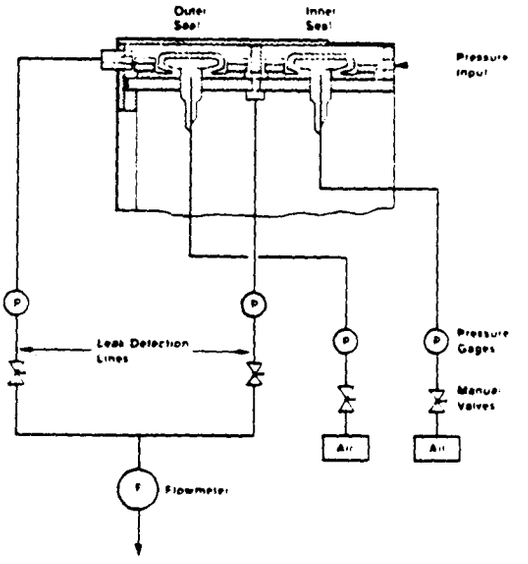

Figure 4. Simplified Schematic of Test Setup
(Note that seals are shown deflated.)

The aged inflatable seals were subjected first to radiation aging and later to thermal aging. The seals received a total gamma radiation dose of 200 Mrad which was applied at a rate of less than 1 Mrad/hr. Also, these seals were thermally aged for 1 week (168 hr) at 250°F. The thermal aging process described above is intended to produce similar properties in the seal material as would be expected after being subjected to a loss of coolant accident at the end of a 10 year life.

Table 3
Test Sequence

Test Series No.	Seal Design	Seal Condition	Loading
1	Old	Unaged	Air, Room Temp. & 400°F
2	Old	Aged	Air, Room Temp. & 300°F
3	New	Unaged	Air, Room Temp. & 300°F,350°F
4	New	Aged	Air, Room Temp. & 300°F

Each series of tests for a given pair of inflatable seals began with room temperature tests. During the room temperature tests, leakage past both seals was limited to a maximum of 10,000 standard cubic feet per day (scfd) so that minimal damage would occur and thus, the same pair of seals could later be tested for elevated temperature conditions.

Separate tests were performed at room temperature in which the initial seal pressure of the unaged seals (Test series 1 and 3) was varied from 50 to as much as 100 psig in increments of 10 psi. Table 4 lists the initial seal pressure levels that were included in

each test series. Because the seals for test series 2 and 4 were aged, there was some concern that any testing at room temperature might damage the seals before the elevated temperature tests. In order to minimize any potential damage, only the 60 psig seal pressure level was tested at room temperature for test series 2 and 4.

To ensure that no damage occurred during any of the room temperature tests, the minimum seal pressure level was retested after completion of all other room temperature tests and the results compared to the first test at that pressure level. No significant change in leakage behavior was observed for test series 1, 2, and 4. However, for test series 3 the leakage behavior for the second 50 psig seal pressure test was much different from the first. Thus, a second "round" of room temperature tests were conducted for test series 3 in which the 50 through 80 psig seal pressure levels were repeated. No further change in leakage behavior was observed after the second round.

For each seal pressure level, the chamber ("containment") pressure was increased from 0 psig until leakage past both seals reached approximately 10,000 scfd.[4] The measured chamber pressure at which leakage of 10,000 scfd occurred for each seal pressure level is provided in Table 4. For test series 1, Figure 5 shows the recorded leakage past both seals as a function of chamber pressure for each seal pressure level. For each pressure level, leakage of 10,000 scfd did not occur until the chamber pressure exceeded the initial seal pressure.

Table 4
Summary of Room Temperature Tests
Test Series 1 Thru 4

Initial Seal Pressure (psig)	Chamber Pressure (psig) for 10,000 scfd Leakage Past Both Seals				
	Test Series 1	Test Series 2	Test Series 3 (Round 1)	Test Series 3 (Round 2)	Test Series 4
50	51.1	----	93.0	58.2	-----
60	65.4	79.0	98.5	76.9	100.5
60C*	----	----	60.1	----	-----
70	79.0	----	104.3	97.4	-----
80	94.7	----	125.1	129.1	-----
90	109.9	----	140.1	-----	-----
90C*	-----	----	92.3	-----	-----
100	129.6	----	-----	-----	-----

*Seal pressure was held constant for these tests.

4. 10,000 scfd is equivalent to 1% mass per day leakage of a $1*10^6$ ft^3 containment.

During round 1 of test series 3, two leakage tests were conducted in which the seal pressure was held constant throughout the test. In this way, the condition could be modeled where the inflation valve (Figure 2) is open during normal operation. For the first of these tests, the seal pressure was set at 60 psig in both seals. As the chamber pressure was increased, the resulting increase in seal pressure was bled off - keeping a constant 60 psig pressure in both seals throughout the test. A similar test was also performed at 90 psig pressure in each seal. The results of these "constant seal pressure" tests are denoted by a "C" suffix on the initial seal pressure listed in Table 4. Figure 6 provides a comparison of the leakage behavior of a constant seal pressure test to a similar test in which the seals were isolated from their pressure source (initial seal pressure level = 90 psig). As shown, in both cases leakage did not begin until the chamber pressure exceeded the initial seal pressure level. However, for the case in which the seals were isolated from their pressure source, leakage did not begin until the chamber pressure was much higher than the initial seal pressure. This improvement can be attributed to the increasing seal pressure caused by increasing chamber pressure when inflatable seals are isolated from their pressure source.

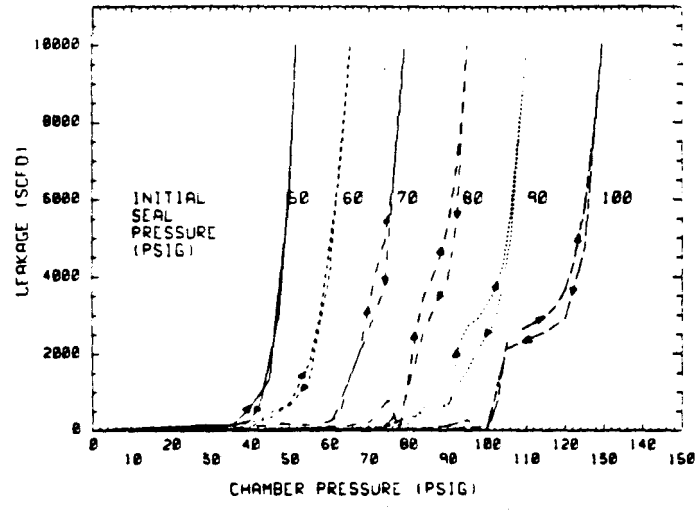

Figure 5. Leakage vs. Chamber Pressure for Various Seal Pressure Levels
Test Series 1 - Seals Isolated From Pressure Source

As earlier mentioned, after completion of all testing at room temperature, leakage tests at elevated temperature were conducted for each pair of seals. Once the inflatable seals test fixture reached the desired temperature, the elevated temperature tests were conducted in basically the same manner as the room temperature tests. The main exception being that, because the elevated temperature tests were destructive in nature, only one seal pressure level could normally be tested for a given pair of seals. The test temperatures and initial seal pressure level for each test series are summarized in Table 5. (All of the elevated temperature tests were conducted with the seals isolated from their pressure source.)

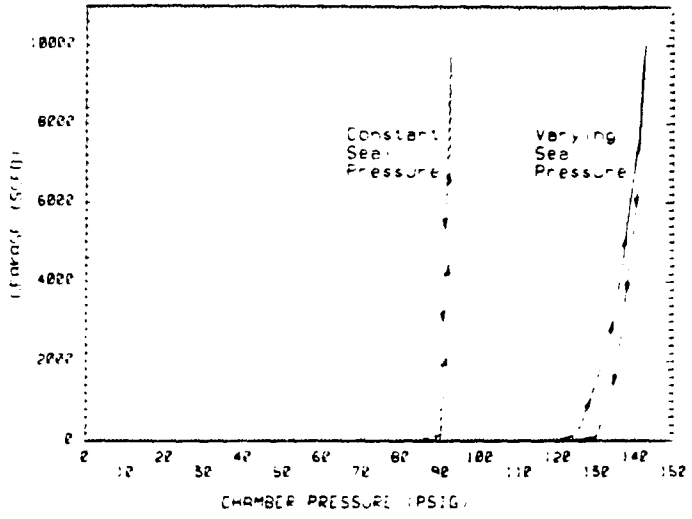

Figure 6. Comparison of Leakage Behavior for Seals Isolated From Pressure Source and for Constant Seal Pressure - Test Series 3 - 90 psig Initial Seal Pressure

While still at room temperature, the seal pressure was set to the level shown in Table 5. A combination of internal heaters and a flow of heated, dry air or steam were used to heat the test chamber and inflatable seals test fixture to the desired test temperature. Once at the test temperature, the chamber temperature was maintained using heated, dry air. The chamber pressure was increased from 0 psig until leakage past both seals exceeded 30,000 scfd - the capacity of the flowmeters. For every test, leakage grew suddenly at failure from less than 5,000 scfd to greater than 30,000 scfd with no appreciable increase in chamber pressure (<2 psi). The internal seal pressure, at elevated temperature, was normally within 5 psig of the chamber pressure when failure occurred. The measured leakage past both seals at 300°F for test series 2, 3, and 4, is shown in Figure 7 as a function of chamber pressure.

Table 5
Summary of Elevated Temperature Tests
Test Series 1 Thru 4

Seal Pressure at Room Temperature (psig)	Test Temperature (°F)	Chamber Pressure (psig) at Failure* of Seals			
		Test Series 1	Test Series 2	Test Series 3	Test Series 4
50	400	132	---	---	---
90	300	---	180	180	138
90	350	---	---	145	---

*Failure is defined as leakage past both seals in excess of 30,000 scfd.

By comparing Tables 4 and 5, it can be seen that, for a given initial seal pressure, a larger chamber pressure was usually necessary to cause significant leakage at elevated temperature than at room temperature. However, it should be noted that, at elevated temperature, significant leakage normally began as a result of a rupture in the seal tube; thus, it was impossible for the seals to reseal once the chamber pressure was reduced. Test series 3 was the only exception. For this test, the seals did not rupture during the 300°F test and thus, they were able to reseal upon reduction of chamber pressure. Because they were still intact, the chamber temperature was increased further to 350°F and another leakage test was performed. Although the seals also remained intact after this test, they ruptured, with virtually no chamber pressure applied, shortly after the temperature was increased to 400°F.

Posttest inspection of the seals revealed that there was no apparent degradation of the EPDM material for test temperatures up to 350°F. However, for test series 1, which was conducted at 400°F, the outer layer of EPDM seemed to have degraded slightly as evidenced by its nonuniform thickness and shiny appearance. Also, an oily residue accompanied the leakage at the conclusion of test series 1. Based on these observations, it appears that appreciable deterioration of the seals begins between 350 and 400°F.

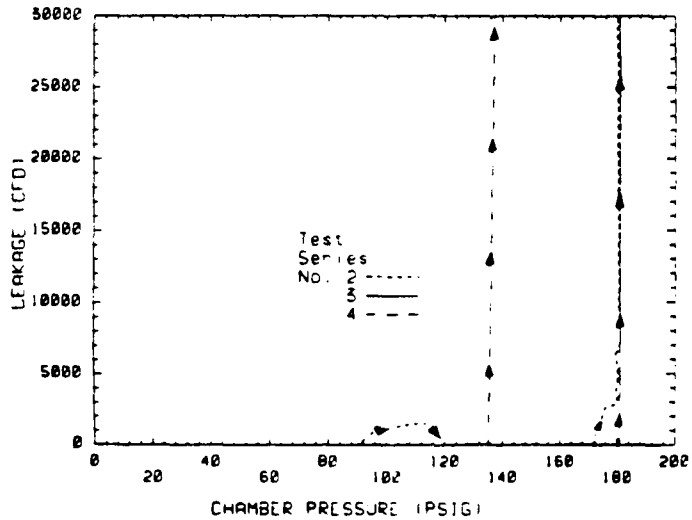

Figure 7. Measured Leakage Past Both Seals Vs. Chamber Pressure at 300°F - Test Series 2, 3, and 4

3.1.3 Developement of Prediction Equations

After completion of the tests, empirically based equations were derived to predict the containment pressure at which leakage can be expected for a given seal pressure and temperature. The prediction equations have been developed for the following range of test parameters.

$$50 \leq P_i \leq 100 \text{ psig}$$
$$70 \leq T_{elev} \leq 400°F$$

where:

T_{elev} = estimated average temperature of seals during accident conditions, °F

P_i = seal pressure under normal operating conditions, psig

Use of the equations beyond these parameters should be performed with caution. The containment pressure at which significant leakage is expected, P_c, may be estimated with the following equation:

$$P_c = \lambda P_s; \text{ not to exceed } P_{max} \quad (1)$$

where:

$$P_{max} = 156.67 - 0.067T_{elev}; \text{ not to exceed 150 psig} \quad (2)$$

= maximum containment pressure without danger of rupturing the inflatable seals; For $T_{elev} \leq 100°F$, P_{max} = 150 psig. For T_{elev} = 400°F, P_{max} = 130 psig.

For ambient conditions:

P_s = P_i = seal pressure under normal operating conditions (i.e., no pressure within containment), psig

For elevated temperatures:

P_s = seal pressure at elevated temperature with no pressure within containment, psig

At elevated temperatures, P_s may be estimated using the ideal gas law and assuming constant volume of the inflatable seals:

P_s = $(TR_{elev}/TR_{amb})(P_{ia}$ @ ambient conditions) - P_a, psig

P_{ia} = absolute seal pressure under normal operating conditions, psia

P_a = atmospheric pressure, psig

TR_{elev} = estimated average temperature of seals during accident conditions, °R

TR_{amb} = seal temperature during normal operating conditions, °R

For constant seal pressure, regardless of seal design:[5]

$$\lambda = 1.0 \qquad (3)$$

For old seal design and assuming that seals are isolated from their internal pressure source:[6]

$$\lambda = 0.006P_s + 0.70 \qquad (50 \le P_s \le 100) \qquad (4)$$

For new seal design and assuming that seals are isolated from their internal pressure source:

$$\lambda = 0.010P_s + 0.70 \qquad (50 \le P_s \le 90) \qquad (5)$$

Because of the limited amount of test data at elevated temperature and the scatter within the available data, the expression for P_{max} intentionally provides lower bound estimates for the predicted chamber pressure at failure at elevated temperatures. Figure 8 provides a comparison of the predicted-to-actual failure pressure ratios for the tested range of initial seal pressures for both the room temperature and elevated temperature tests.

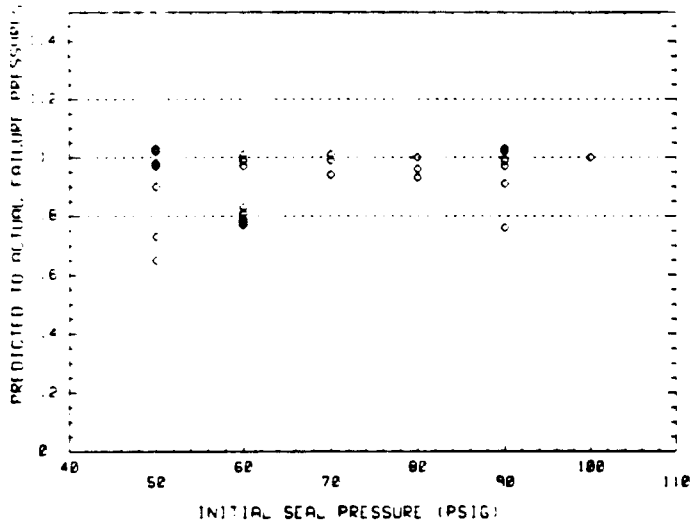

Figure 8. Comparison of Predicted-to-Actual Failure Pressures for the Test Range of Initial Seal Pressures

In summary, results of the inflatable seals tests have shown that, regardless of the position of the inflation valve (Figure 2), applied seal aging, seal design, or normal operating seal pressure, significant leakage past the seals will not occur until the containment pressure exceeds the normal operating seal pressure. If the seals are isolated from their pressure source, significant leakage may not begin until the containment pressure is considerably greater than the normal operating seal pressure. Also, because there were signs of a

---

5. Assumes that an open pathway exists between the seal tube and the accumulator tank.

6. Assumes that a closed valve isolates the seal from the accumulator tank.

breakdown in the seal material for temperatures in excess of 350°F, use of inflatable seals in environments greater than 350°F should be done with caution.

3.2 Bellows

The information presented in this section has been obtained through extensive interviews with experienced bellows designers and manufacturers. Also, the summary of containment penetrations presented in References 16 and 17 provided much of the geometric details that will be discussed. Not all containment penetrations that employ bellows have been surveyed. However, it is believed that an adequate survey has been conducted to understand the general purpose of containment bellows and to envelope all possible containment bellows designs.

Bellows are employed at most process piping penetrations of steel containments in order to minimize the piping loads applied to the containment shell while maintaining the containment pressure boundary. Process piping bellows vary in size from 6 to around 60 inches in diameter. They are normally constructed of two plies of SA240, Type 304, stainless steel which are separated by a thin wire mesh (≈0.010-inch diameter). The primary purpose of the redundant outer ply is to provide a means to check for leakage of the bellows by pressurizing the space between plies and noting any drop in pressure. Figure 9 illustrates a typical application of bellows at a process piping penetration.

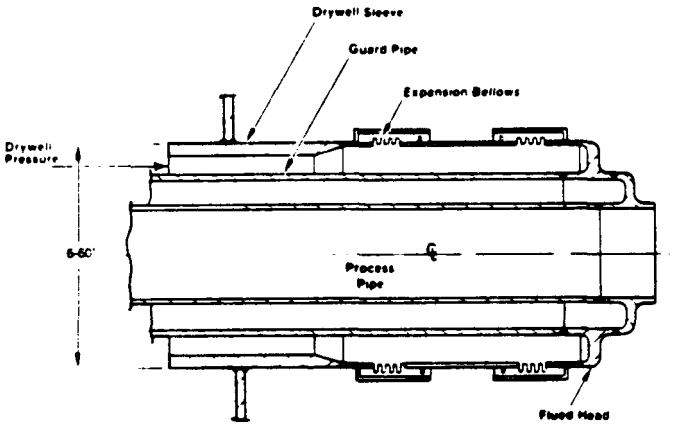

Figure 9. Typical Application of Process Piping Bellows

Bellows are also used at the penetration of each vent line into the suppression chamber in BWR Mk-I containments. Vent line bellows range in diameter from about 65 to as much as 125 inches. The majority of the vent line bellows are one ply; approximately 10% are two-ply. The vent line bellows are also constructed of SA240, Type 304 stainless steel. Figure 10 shows a typical application of bellows at the penetration of a vent line into the suppression chamber of a Mk-I containment.

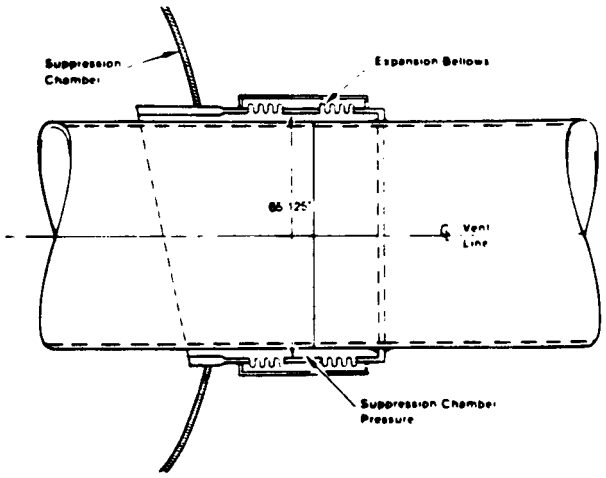

Figure 10. Typical Application of Vent Line Bellows

Containment penetration bellows are designed to absorb differential movement between the containment shell and the pipe to which they are attached. The design movements result from the following conditions: normal operation, safe shutdown earthquake (SSE), and loss of coolant accident (LOCA). In most cases, the bellows design movements were obtained by summing the maximum deformations associated with each of these conditions as if they occurred simultaneously. The provisions included in the Standards of the Expansion Joint Manufacturers Association (EJMA) [18] were used for the bellows design. Normally, the bellows were designed to resist about 5,000 cycles of the above "worst case" loading. Also, each ply was sized to resist the full containment design pressure. Using the EJMA approach, a minimum factor of safety of four against burst due to internal pressure only must be obtained. Thus, especially for the two-ply bellows, a considerable margin should exist between normal containment design conditions and those conditions that would cause a failure of the bellows pressure boundary.

In the event of a severe accident, pressure and temperature conditions within containment may reach levels which are well beyond the design basis. In most cases, radial growth of containment due to internal pressure imposes axial compression on the bellows. (There are a few cases in which radial growth of containment elongates the bellows.) For cylindrical containments, the bellows must also absorb lateral deformation caused by the vertical growth of the containment shell due to increasing temperature and the "uplift" caused by the pressure acting on the dome. If the containment pressure is sufficient to cause general yielding in the hoop direction, the radial growth increases rapidly for small additional increases in pressure. Figure 11 illustrates, in generic terms, the increase in axial compression and lateral deformation that will be imposed on a bellows for increasing containment pressure. As shown, if the containment pressure is high enough, it is possible that the bellows could become fully compressed (i.e., each convolution is fully closed so that there is no remaining flexibility of the bellows). Upon reaching full compression, it is extremely likely that a tear in the bellows will occur opening a potentially large leak path through the containment pressure boundary.

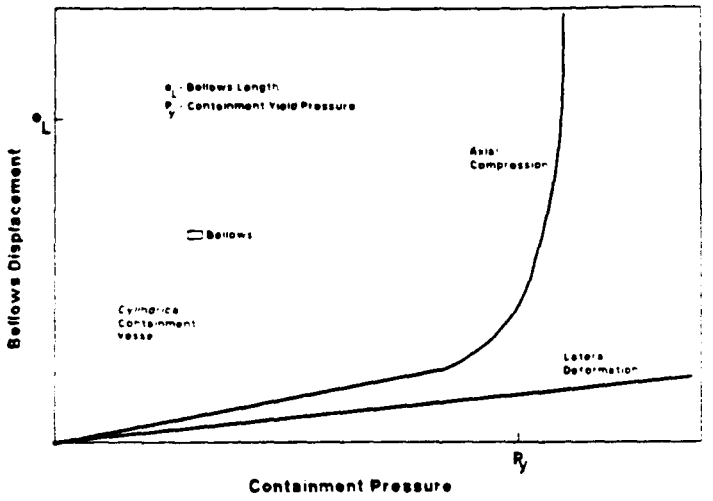

Figure 11. Bellows Deformations Caused By Increasing Containment Pressure

An extensive review of bellows-related literature has been conducted and several bellows manufacturers and designers have been interviewed. However, at this time, there has been no known past research efforts in which bellows have been subjected to the extreme loading conditions that might occur during a severe accident.

At this point, there are a number of unanswered questions regarding the performance of containment bellows during a severe accident.

1) Are containment bellows capable of being fully compressed when subjected to simultaneous lateral deformation, internal pressure, and elevated temperature without developing a tear in the bellows material or in the connection of the bellows to the end spool?

2) Can containment bellows withstand the postulated combinations of elongation, lateral offset, external pressure, and elevated temperature without a failure of the bellows pressure boundary?

If containment bellows cannot remain leaktight under these conditions, then methods must be developed to predict the possible deformation and pressure conditions that would likely cause a failure of the bellows pressure boundary.

Currently, plans are being developed to conduct a series of tests in which representative bellows are subjected to postulated severe accident loadings. During the tests, various combinations of internal and external pressure, axial compression, elongation, and lateral deformation will be applied to typical bellows geometries. The magnitudes of deformations to be applied will be determined from global shell analyses of typical containments at the position of the most critical bellows. The goal of these tests is to develop methods to predict the pressure and deformation conditions that will likely cause a tear in the bellows, which could produce a large leak path through the containment boundary.

3.3 Equipment Hatch Tests

A series of tests are underway on the pressure-unseating equipment hatch in the 1:6-scale reinforced concrete model (equipment hatch 'B1'). The tests are designed to provide engineering data that can be used to validate analytical approaches to predict leakage from pressure-unseating equipment hatches and drywell heads. Specifically, information on the effects of bolt preload, bolt stiffness, gasket material, gasket aging, and temperature on the containment pressure at which significant leakage initiates and on the leak rates that arise is being obtained.

Equipment hatch 'B1', which is shown schematically in Figure 12, uses a sealing arrangement that is typical of many pressure-unseating equipment hatches and drywell heads. The bolts are used to attach the cover to the penetration sleeve and preload the sealing surfaces in compression. A double tongue and groove configuration is used to form the seal. Typically, preload is specified such that separation of the sealing surfaces will occur in the range of 1.1 to 1.5 times the containment design pressure. However, the gasket can still maintain a seal for some positive separation, the magnitude of which depends on the compression set retention and containment pressure and temperature.

An analytical method has been developed to estimate the pressure and temperature at which significant leakage first occurs and the rate of leakage for pressure and temperature conditions above this level. The test results will be used to improve and validate the analysis. The analytical method can be broken into three steps:

1. The structural response, in particular, the separation displacement (relative motion of the sealing surfaces) is determined based on a strength of materials approach.

2. The maximum separation displacement for which the gasket can prevent leakage is evaluated using an empirical parameter for gasket performance, S_p, which is a measure of the available springback. S_p depends on the sealing configuration and geometry, aging history of the gasket, gasket material, and accident temperature.

3. Risk significant leak rates are calculated from fluid mechanics equations for choked flow through a duct of known area, where the area is determined from steps 1 and 2.

This approach leads to the following set of equations [19]:

$$q = \sqrt{\frac{\gamma}{R}} \quad \frac{p_1 A_1 M_1}{\sqrt{T_1}} \tag{6}$$

where q is the mass flow rate, γ is the ratio of specific heats, R is the gas constant, and p_1, A_1, M_1, and T_1 are the absolute pressure, leak area, mach number, and absolute temperature at the inlet. Furthermore,

$$p_1 = p(1 + M_1^2)^{-3.5} \tag{7}$$

$$T_1 = T_g(1 + M_1^2)^{-1} \tag{8}$$

$$A_1 = 2\pi rg \tag{9}$$

$$M_1 = \begin{cases} 0 & \text{for } g = 0 \\ f(fL_{max}/2g) & \text{for } g > 0 \end{cases} \tag{10}$$

where p is the absolute containment pressure, T_g is the containment gas absolute temperature, r is the inside radius of the equipment hatch sleeve (or drywell head flange), g is the gap between the sealing surface and the gasket (the gap is assumed to be uniform, which is recognized as a rough approximation at best), f is the friction coefficient (typically equal to .02), and L_{max} is the length of the flow path (approximately 1.0 inch for equipment hatch 'B1'). The function f in Eq. (5) is one of the Fannow Line Flow functions, which are tabulated in Reference 20. Eq. (1) is valid only when $p^* > p_a$, where p^* is the absolute exit pressure and p_a is the atmospheric pressure. The exit pressure can be determined from the ratio of p_1/p^* given by the Fannow Line Flow Functions, where p_1 is given by Eq. (2).

The structural response is calculated from equations appearing in Reference 21, with some modifications to account to account for temperature and Poisson effects. The gap, g, separation displacement, s, and separation pressure, p_s, are given as:

$$g = \begin{cases} 0 & \text{for } s < S_p \\ s - S_p & \text{for } s > S_p \end{cases} \tag{11}$$

$$s = \begin{cases} 0 & \text{for } p < p_s \\ \pi r^2(p-p_s)\left[\frac{1}{k_B} + \frac{2\nu}{k_F}\right] & \text{for } p > p_s \end{cases} \tag{12}$$

$$p_s = \frac{\frac{k_B + k_F}{k_F}F_i + k_B(\epsilon_{TF} - \epsilon_{TB})L}{\left(1 + 2\nu\frac{k_B}{k_F}\right)\pi r^2} \tag{13}$$

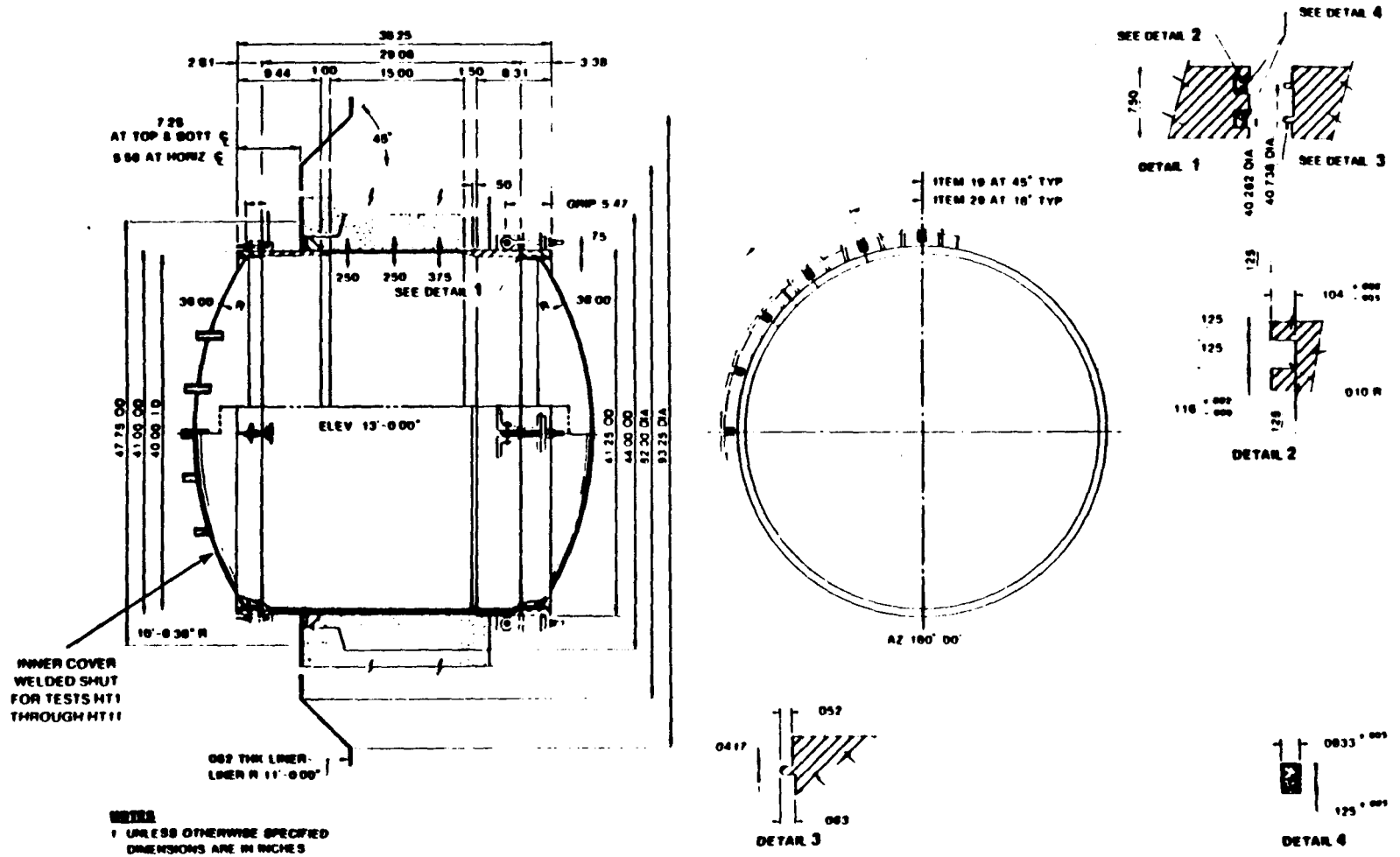

Figure 12. Schematic of Equipment Hatch 'B' in 1:6-Scale Reinforced Concrete Containment Model

where S_p is the available gasket springback, k_B is the elastic axial bolt stiffness (which should be obtained from tensile tests), k_F is the elastic axial flange stiffness, ν is Poisson's ratio, F_i is the mechanical bolt preload, ϵ_{TF} and ϵ_{TB} are the average thermal strains in the flange and bolt, respectively, and L is bolt grip length. For typical containment applications, k_B/k_F is around 1%; thus, the above calculations are relatively insensitive to variations in the value of k_F. The available gasket springback can be approximated from the cross-sectional dimensions of the gasket, tongue and groove geometry and the gasket compression set retention; however, other factors, such as thermal expansion, pressure, and temperature may also affect gasket performance. Testing is expected to provide insight into the importance of these factors.

It should also be noted that ϵ_{TF} and ϵ_{TB} are temperature dependent material properties; for a given material:

$$\epsilon_{TF} = f(T_F) \tag{14}$$

$$\epsilon_{TB} = f(T_B) \tag{15}$$

where T_F and T_B are the average temperatures of the flange and bolts, respectively. The function f in Eqs. (9) and (10) may be represented as a linear function with the coefficient of thermal expansion as the proportionality constant; however, the above formulation is more general.

The current test matrix is given in Table 6. The test matrix was designed to provide the following information:

1. The effect of different combinations of pressure and temperature(to simulate different accident scenarios) on separation pressure, separation displacement, and leakage.

2. The effect of different gasket materials on leakage.

3. The effect of gasket aging history on leakage.

4. The effect of bolt preload on separation pressure.

5. The effect of bolt stiffness (number of bolts) on separation displacement.

The equipment hatch has been instrumented with a large number of high temperature, weldable strain gages, capacitance displacement probes, thermocouples, flowmeters, and pressure transducers, as shown schematically in Figures 13 and 14. An acoustic emissions system is also used to help detect the initiation and location of leakage. Before testing, gaskets are thermally aged in place as specified in Table 6. Castings are made of the cross-sectional shape of the gasket before and after aging and again after testing to determine the gasket available springback. After the bolts are preloaded to their specified value, testing is conducted by stepwise pressurization using nitrogen gas, with data recorded after each pressure increment.

Tests HT1 through HT4 have been completed and quick look reports have been issued [22,23]. The results are briefly summarized here. All of these tests were conducted at ambient temperature, so pressure is the only loading. Figure 15 shows the comparisons between the calculated and measured separation displacement for tests HT1 through HT4. These figures also indicate the available springback and the pressure at which significant leakage was first detected. Table 7 also provides an overview of the comparison between calculated and measured results.

The following observations are made based on the results of tests HT1 through HT4:

- Although the actual hatch behavior is not uniform, the average response of the hatch (around the circumference), including the pressure at which preload is overcome, compares favorably with calculations.

- The mean available springback is a reasonably accurate measure of gasket performance. In three of the four tests, significant leakage first occurred when the separation displacement was in the range of the mean available springback (based on actual measurements before testing) plus or minus one standard deviation.

- The mean available springback tends to underestimate the sealing capability of aged gaskets and tends to overestimate the sealing capability of unaged gaskets.

- Within the specified tolerances on the gasket and groove cross-sectional dimensions of equipment hatch B1, the available springback for a gasket with zero compression set retention may vary from 27 to 51 mils. In these tests, the actual dimensions are known; however, in applications, the dimensional tolerances represent an important source of uncertainty in characterizing the available springback, a parameter to which the results are particularly sensitive. (Another important source of uncertainty is the actual exposure of gaskets to temperature and radiation during their service life.)

- Once leakage begins, the leak rate determined by the proposed method tends to greatly overestimate the actual leak rate. The agreement is poor probably because the analytical method assumes the separation displacement increases uniformly and the available springback is uniform; these assumptions are not accurate.

These tests provide confirmatory evidence that the gross response can be used to predict the initiation of significant leakage when the available springback is used as the gasket performance parameter. In practice, the calculated results are subject to large uncertainty because important parameters such as the bolt stiffness, bolt preload, and available springback are not as well characterized as in these tests. A probabilistic approach should be used in actual applications by assigning appropriate distributions to the values of these parameters and then using a simulation technique.

Table 6
Revised Test Matrix for Investigating
the Leakage Potential of a Pressure-Unseating Equipment Hatch

Test Designator	Gasket Material	Aging Duration[1] (hours)	Bolt Preload (kips)	Number of Bolts	Test Load[2]
HT1	SI	144	57.2	10	A
HT2	EP	Unaged	68.7	10	A
HT3	EP	Unaged	91.5	20	A
HT4	EP	168	91.5	20	A
HT5	EP	Unaged	91.5	20	B
HT6	EP	144	91.5	20	B
HT7	EP	168	114.4	20	B
HT8	SI	168	91.5	20	B
HT9	EP	Unaged	91.5	20	C
HT10	EP	144	91.5	20	C
HT11	SI	144	91.5	20	C

Notes:

1. Gaskets will be aged in-place at 300°F for the indicated time to simulate both radiation and thermal aging. Data from Reference 21 indicates that compression set retention of EP and SI seals is most sensitive to radiation aging. Exposure to as little as 50 Mrads results in compression set retention of 75% for EP and 90% for SI. Typically, a radiation dose of 200 Mrads has been used in other experiments and, although it may represent an overtest, the compression set retention is about 95% for EP and about 97% for SI at this level of exposure. Since only thermal aging is practical for the equipment hatch tests, the aging time (and possibly temperature also) should be adjusted to achieve compression set retention of the gaskets between 80% and 95%. Dimensional measurements of the gasket will be made three times: when the gaskets are first placed in the grooves and before the cover has been installed; before pressure testing and after the cover has been in place with the bolts torqued to 40 ft-lbs for at least one day (or, if applicable, after aging); and after pressure testing (unless the gaskets are not intact).

2. A - Stepwise pressurization at ambient temperature.
   B - Stepwise pressurization and heating; temperature held equal to the steam saturation temperature at the current pressure.
   C - Hold gas temperature at level sufficient to maintain the gasket at or above its degradation temperature as defined in Reference 9 for at least two hours; maintain temperature and initiate a stepwise pressurization.

   For all three cases, pressurization with nitrogen will continue until significant leakage is detected or until the maximum allowable pressure, as defined in the SOP, is reached, whichever comes first.

Table 7
Summary of Calculated and Measured Behavior

Test No.	HT1	HT2	HT3	HT4
Maximum Test Pressure (psig)	95	115	200	180
Leak Rate at Maximum Test Pressure (scfm)				
Measured	25	30	13	0[2]
Calculated	80	0	0	570
Leakage Initiation Pressure[1] (psig)				
Measured	90-95	110-112	195-197	>180
Calculated	93	120	222	166
Separation at Leakage Initiation[3] (mils)				
Measured[4]	25	36	35	32
Calculated	23	32	33	28
Available Springback (mils)				
Mean	22	39	39	25
Standard Deviation	4	6	6	2

Notes:
1. Measured value arbitrarily defined as pressure at which leakage first exceeded 5 scfm; calculated value corresponds to the initiation of leakage.
2. No leakage was measured up to the maximum test pressure of 180 psig. HT4 was terminated at this point because of large inelastic strains in a few bolts.
3. These values are based on the upper end of the range of pressures listed for initiation of leakage.
4. Average of all 20 displacement transducers.

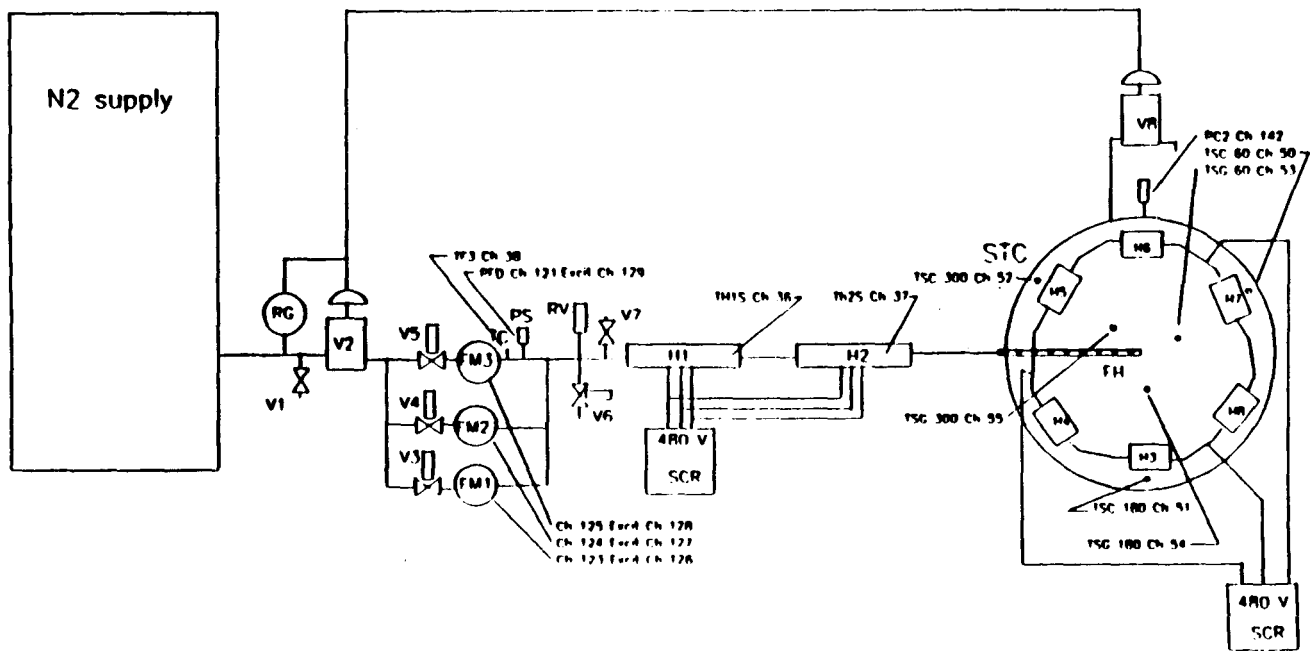

Note: 1 1/2 in. schedule 80 pipe and fittings

Figure 13. Schematic of Pressurization and Heating Instrumentation

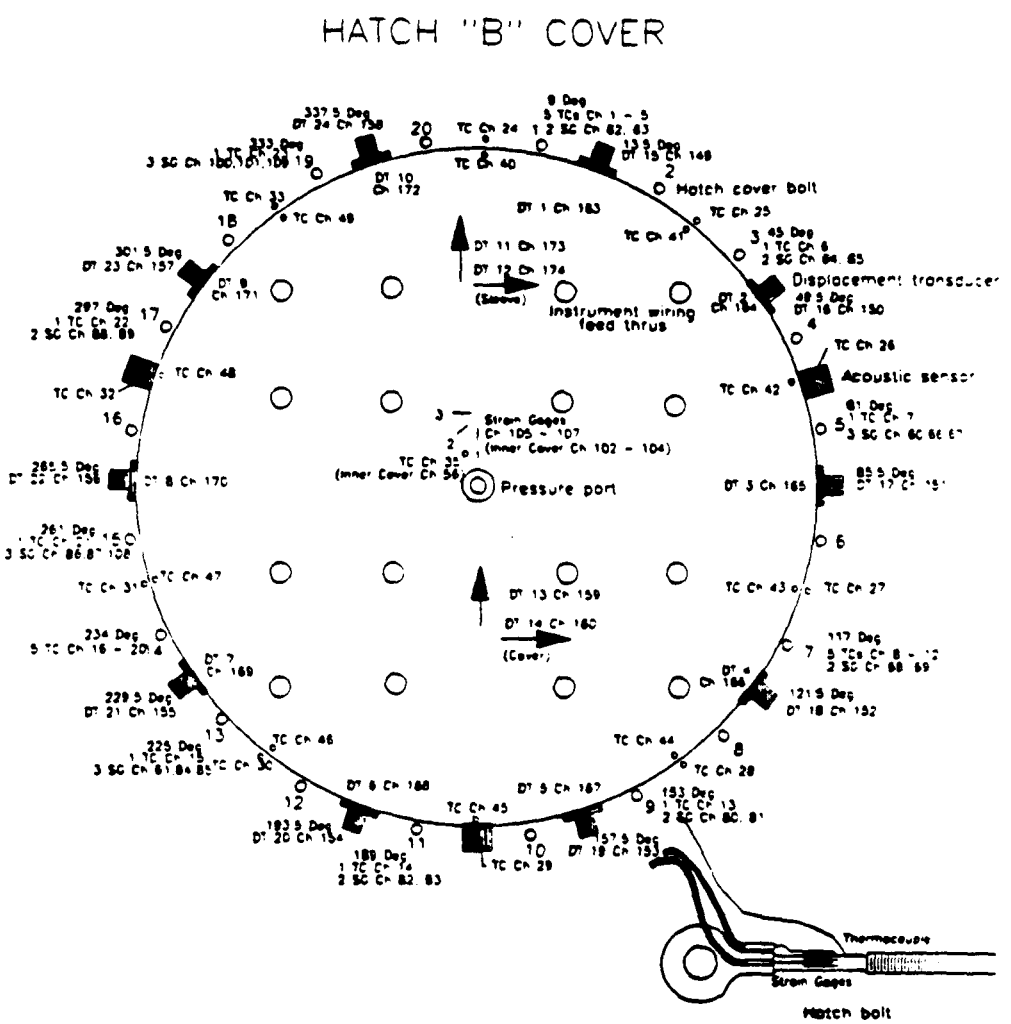

Notes:

1.) Two strain gages and one thermocouple on all odd numbered bolts with five thermocouples on bolts 1, 7, and 14.
2.) Bolts 5, 13, 15, and 19 have an additional strain gage opposite the top gage in the illustration. (Ch 60, 61, 108, 109)
2.) One thermocouple inside and one outside at ten locations between bolts, near sealing surface.
3.) Displacement transducers inside and out at ten locations.
4.) Acoustic sensors at three locations.

Figure 14. Schematic of Instrumentation on Bolts and Near Sealing Surfaces

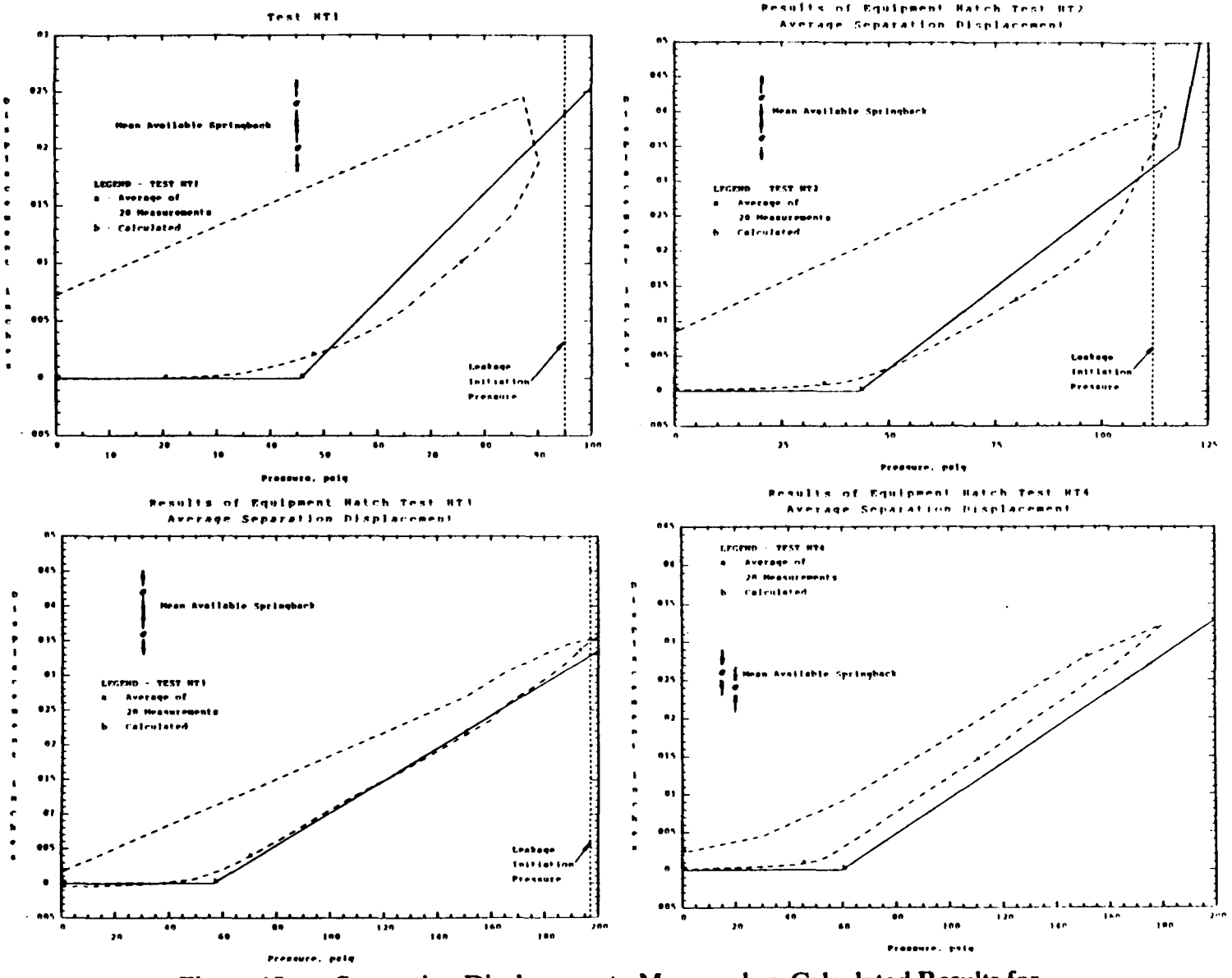

Figure 15. Separation Displacement: Measured vs. Calculated Results for Ambient Temperature Tests

4.0 SUMMARY

Each of the Sandia containment penetration programs have been briefly described. For the completed programs, guidelines have been presented to estimate the pressure and temperature conditions that would likely produce a failure of the pressure boundary of each type of penetration. Because there are considerable variations in the penetration designs and because of the limited number of tests conducted, each program should be carefully examined and thoroughly understood before applying the analytical methods and test results to the evaluation of other similar penetration designs.

The final goal of the Containment Integrity Programs at Sandia is to develop a complete methodology to estimate the capacity associated with each potential failure mode of the containment pressure boundary. The containment pressure boundary is composed of both the shell and many mechanical and electrical penetrations. The capacity of the containment boundary can be estimated as simply the failure mode with the lowest predicted pressure capacity at elevated temperatures.

5.0 REFERENCES

[1] Clauss, D. B., "Comparison of Analytical Predictions and Experimental Results for a 1:8-Scale Steel Containment Model Pressurized to Failure", NUREG/CR-4209, SAND85-0679, Sandia National Laboratories, Albuquerque, NM, July 1985.

[2] Cochrell, R. C., (ed.), Proceedings of the Fourth Workshop on Containment Integrity, Session E (Analyses Associated with Sandia 1:6-Scale Model Test), NUREG/CP-0095, SAND88-1836, Sandia National Laboratories, Albuquerque, NM, October 1988.

[3] Horschel, D. S., and Blejwas, T. E., "An Analytical Investigation of the Response of Steel Containment Models to Internal Pressurization," Transactions of the Seventh International Conference on Structural Mechanics in Reactor Technology, Volume J6/4, Chicago, IL, August 1983.

[4] Horschel, D. S., "Experimental Results from Pressure Testing a 1:6-Scale Nuclear Power Plant Containment," NUREG/CR-5121, SAND88-0906, Sandia National Laboratories, Albuquerque, NM, 1988.

[5] Clauss, D. B., (ed.), "Round Robin Pretest Analyses of a 1:6-Scale Reinforced Concrete Containment Model Subject to Static Internal Overpressurization," NUREG/CR-4913, SAND87-0891, Sandia National Laboratories, Albuquerque, NM, April 1987.

[6] Clauss, D. B., (ed.), "Round-Robin Analysis of the Behavior of a 1:6-Scale Reinforced Concrete Containment Model to Failure: Posttest Evaluations," NUREG/CR-5341, SAND89-0349, Sandia National Laboratories, Albuquerque, NM, October 1989.

[7] Horschel, D. S., "Design, Construction, and Instrumentation of a 1/6-Scale Reinforced Concrete Containment Building," NUREG/CR-5083, SAND88-0030, Sandia National Laboratories, Albuquerque, NM, 1988.

[8] Steele, R., Jr. and Watkins, J. C., "Containment Purge and Vent Valve Test Program Final Report," NUREG/CR-4141, EG&G Idaho, Inc., Idaho Falls, Idaho, September 1985.

[9] Brinson, D. A., and Graves, G. A., "Evaluation of Seals for Mechanical Penetrations of Containment Buildings," NUREG/CR-5096, SAND88-7016, Sandia National Laboratories, Albuquerque, NM, 1988.

[10] Bridges, T. L., "Containment Penetrations Elastomer Seal Leak Rate Tests," NUREG/CR-4944, SAND87-7118, Sandia National Laboratories, Albuquerque, NM, July 1987.

[11] Clauss, D. B., "Severe Accident Testing of Electrical Penetration Assemblies," NUREG/CR-5334, SAND89-0327, Sandia National Laboratories, Albuquerque, NM, 1989.

[12] Keck, J. D., and Thome, F. V., "Electrical Penetrations Assemblies Severe Accident Testing," Proceedings of the Intl. Topical Meeting on Operability of Nuclear Power Systems in Normal and Adverse Environments, pp 181-186, September 29-October 3, 1986.

[13] Julien, J. T., and Peters, S. W., "Leak and Structural Test of Personnel Airlock for LWR Containments Subjected to Pressures and Temperatures Beyond Design Limits," NUREG/CR-5118, SAND88-7155, Sandia National Laboratories, Albuquerque, NM, May 1989.

[14] Clauss, D. B., Parks, M. B., Weatherby, J. R., and von Riesemann, W. A., "Progress Report on the Containment Integrity Programs," Proceedings of the 16th Water Reactor Safety Meeting, Washington, DC, 1988.

[15] Parks, M. B., "Evaluation of the Leakage Behavior of Inflatable Seals Subject to Severe Accident Conditions," NUREG/CR-5394, SAND89-1454, Sandia National Laboratories, Albuquerque, NM, 1989.

[16] Bump, T. R., et al., "Characterization of Nuclear Reactor Containment Penetrations - Preliminary Report," NUREG/CR-3855, SAND84-7139, Sandia National Laboratories, Albuquerque, NM, June 1984.

[17] Shackelford, M. H., et al., "Characterization of Nuclear Reactor Containment Penetrations - Final Report," NUREG/CR-3855, SAND84-7180, Sandia National Laboratories, Albuquerque, NM, January 1985.

[18] Standards of the Expansion Joint Manufacturers Association, Fifth Edition, Tarrytown, NY, 1980.

[19] Hickox, C. E., "Gas Leakage Rate Analysis for Scale Model LWR Containment Structure," Internal Memorandum to D. B. Clauss, 6442, Sandia National Laboratories, April 16, 1986.

[20] John, J. E. A., Gas Dynamics, Allyn and Bacon, Boston, 1969.

[21] Shigley, J. E., Mechanical Engineering Design, McGraw-Hill, New York, 1977, pp 240-250.

[22] Orwick, P. E., "Aging Characteristics of Presray Seal and Gasket Material," Presray report, March 1986.

[23] Clauss, D. B., "Quick Look Report for Equipment Hatch Test HT1," Internal Memorandum to Distribution, Sandia National Laboratories, Albuquerque, NM, June 16, 1989.

[24] Clauss, D. B., "Quick Look Report for Equipment Hatch Tests HT1 Through HT4," Internal Memorandum to Distribution, Sandia National Laboratories, Albuquerque, NM, October 6, 1989.